Conference paper

Károly Lázár*

Redistribution of iron ions in porous ferrisilicates during redox treatments

DOI 10.1515/pac-2016-1026

Abstract: Relocation of iron ions in microporous Fe-FER, (Al + Fe)-FER, Fe-MFI (FER: ferrierite, MFI: silicalite) and in mesoporous Fe-MCM-41 ferrisilicate (MCM: Mobile Crystalline Material) samples was followed during redox treatments primarily by tool of the in situ Mössbauer spectroscopy. Coexistence of various Fe^{3+} and Fe^{2+} species is demonstrated. In microporous Fe-FER and Fe-MFI existence of combined μ-oxo iron dimers, Fe^{3+}_{FW}-O-Fe^{2+}_{EFW} can be proposed. The presence of these dimers can easily be correlated with catalytic effect shown in certain oxidation processes. Structural rearrangement can also be revealed in mesoporous Fe-MCM-41 which result in improvement of catalytic performance in CO oxidation.

Keywords: dinuclear μ-oxo iron; framework and extra-framework iron; in situ Mössbauer spectroscopy; μ-oxo iron dimers; porous ferrisilicates; SSC-2016.

Introduction

Transition metal ions in porous nano- and mesoporous systems may change their positions in correspondence with the applied treatments. In microporous zeolites this feature has been known since long time [1]. Redox treatments may enhance the process, since the charge of various involved species may change [2]. Further on, in cases of iron and copper ions even a simple evacuation may result in a change of the location. Namely, irreversible autoreduction may occur, when transition metal ions are removed from the tetrahedral framework sites to extra-framework positions [3]. The process is irreversible, the formed reduced ions have larger radii than the original tetrahedrally coordinated species do (eg. 77 pm for Fe^{2+} and 63 pm for Fe^{3+}[4]).

The actual distribution of transition metal ions among tetrahedral framework (FW) and more open charge compensating extra-framework (EFW) sites plays important role. In particular, catalytic properties depend strongly on the FW/EFW distribution. Namely, transition metal ions in FW sites usually may exhibit Brønsted acidity (with proton transfer) [5], whereas EFW sites exhibit Lewis acidity. The change of the FW/EFW distribution due to reduction/oxidation (or to the catalyzed process itself) may result in the change of the further catalytic performance.

Ferrisilicates catalyze various processes [6, 7]. Among them oxygen transfer reactions are frequently promoted. In one part single iron site catalysis (one EFW Fe ion, with possible assistance of FW aluminum, or EFW AlO^+) has been proposed for transferring oxygen [8, 9]. On the other part possible role of μ-oxo (Fe-μ-O-Fe and Fe-μ-(O_2)-Fe) dimers is also emphasized. These μ-oxo Fe-O-Fe dimers are usually formed from EFW iron ions, introduced in a second stage after the synthesis [10–12]. However, combined Fe-O-Fe dimers may also be formed, from FW position for one iron ion and EFW position for the second iron ion of the dimer. This type of dimers is scarcely described in the literature [13].

Article note: A collection of invited papers based on presentations at the 12th Conference on Solid State Chemistry (SSC-2016), Prague, Czech Republic, 18–23 September 2016.

***Corresponding author: Károly Lázár,** Department of Nuclear Analysis, Centre for Energy Research, Hungarian Academy of Sciences, 29 – 33. Konkoly Thege M. 1121, Budapest, Hungary, e-mail: lazar.karoly@energia.mta.hu

© 2017 IUPAC & De Gruyter. This work is licensed under a Creative Commons Attribution-NonCommercial-NoDerivatives 4.0 International License. For more information, please visit: http://creativecommons.org/licenses/by-nc-nd/4.0/

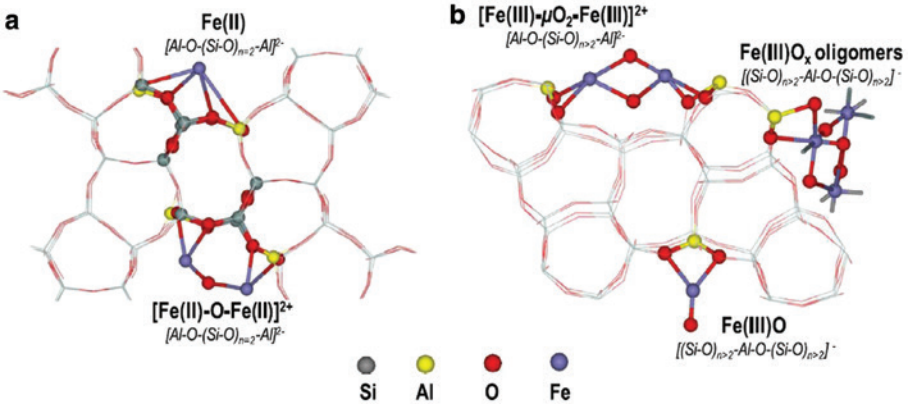

Fig. 1: Possible locations available for EFW Fe^{2+} (a left) and Fe^{3+} (b right) species in ZSM-5. Mono- di-, and oligonuclear species are shown. (Reproduced with permission from [14]).

For better illustration, possible locations available for EFW iron in ZSM-5 structure are shown in Fig. 1 [14].

The various iron containing species are anchored to the framework via Al_{FW}-O-Fe_{EFW} bridges, originating from tetrahedral Al FW sites. It is seen that ample space is available around iron ions where the coordination sphere of ions can be filled with other molecules, either with reactans or e.g. with H_2O, $(OH)^-$ etc. It should be mentioned that primary structures of FER and ZSM-5 are similar (e.g. the diameter of the ten-membered channels).

In the present communication three examples are shown from studies on microporous ferrisilicates, with emphasis on detection of possible formation and redistribution of the combined Fe_{FW}-O-Fe_{EFW} dinuclear centers during reduction – oxidation cycles. Redistribution of iron ions among FW and EFW sites is clearly manifested in the reported cases (Fe-FER, (Fe + Al)-FER, and Fe-MFI; FER: ferrierite, MFI: silicalite). For comparison of properties of iron ions in microporous zeolite structures with iron in mesoporous ferrisilicates a further example (Fe-MCM-41, MCM: Mobile Crystalline Material) is also presented. Furthermore, beside redox cycles, relocation of iron may take place when certain damage of the crystal structure proceeds. Curiously, the original activity in certain reactions may be retained in a great extent even after a partial collapse of the structure. An example for this instance is also illustrated in the decomposition of N_2O.

The primary method used for these studies was ^{57}Fe Mössbauer spectroscopy which is particularly sensitive tool to detect coordination and oxidation state of iron ions. The method has successfully been applied in several instances for studying states of iron in zeolites [8, 14–16].

Experimental

Samples

Fe-FER and (Al + Fe)-FER samples were synthesized hydrothermally with pyrrolidine template. The Si : Fe ratio was 16 in the first sample. In the second sample the Si/(Al + Fe) ratio was the same, 16, with an Al : Fe = 3 : 1 ratio. Further details of synthesis and sample chracterization are described in [17].

Fe-MFI sample containing both Fe^{3+} in FW and Fe^{2+} in EFW siting was synthesized in two stages. First FW iron was introduced in hydrothermal synthesis using ^{57}Fe in Si/Fe ratio ~ 200. Further details of the first stage are described in [18]. In the subsequent stage Fe^{2+} was intruduced from ethanolic solution under inert atmosphere. The average iron content of the sample was determined by atomic absorption spectroscopy after dissolution, Si/Fe ~ 50 ratio was found. Thus, a nominal FW : EFW = 1 : 3 ratio can be estimated for this sample. Further details on the preparation and on catalytic test for N_2O decomposition are described in [19].

MCM-41 sample was synthesized hydrothermally using $^{57}Fe_2(SO_4)_3$ iron source, with Si: Fe = 1: 140 ratio and cetyltrimethylammonium bromide as structure directing agent. Details of the synhesis are descibed in [20].

The principal method used for characterization: in situ Mössbauer spectroscopy

^{57}Fe Mössbauer spectroscopy is a particularly sensitive technique to analyze coordination and oxidation states of iron. To identify the various coordination and oxidation states of iron in porous ferrisilicates an excellent compilation of isomer shift (δ) and quadrupole splitting (Δ) data based on spectra of a broad veriety of ferri- and ferrosilicate minerals can be used [21, 22]. Our studied micro- and mesoporous ferrisilicates were exposed to redox treatments under different conditions in an in situ cell described in [23]. Treatments were usually performed in sequence on one sample and spectra were recorded after each corresponding stages.

Results and discussion

Studies in reduction oxidation cycles

For interpretation of performance and stability of ferrisilicates in catalytic processes it is worth to perform redox cycles. In a rough approach reducing atmospheres may correspond to the conditions provided by the organic reactants, whereas the oxidation may refer to the activation of catalysts. During these reversal of atmospheres relocation of iron among possible sites may proceed.

Fe-FER

This sample contained only silicon and iron, i.e. aluminum was not present in it. Thus, charge compensation of tetrahedral Fe^{3+}_{FW} sites can be provided with extra-framework iron ions and with Brønsted acidic H^+ protons. Mössbauer spectra were collected on Fe-FER samples with Si/Fe = 16 ratio. The first step, the hydrothermal synthesis resulted primarily in the inclusion of Fe^{3+} ions into tetrahedral FW sites. In the course of the further treatments a part of iron was relocated to EFW sites, as in situ Mössbauer spectra attest (Fig. 2 and Table 1).

First it should be noticed that the evacuation at 620 K after calcination results in the removal of adsorbed water from the vicinity of the FW substituted iron and Brønsted acidic sites form with H^+ charge compensation (Fig. 2b). The distorted tetrahedral symmetry results in appearance of large quadrupole splitting for the FW iron ions (Δ = 1.97 mm/s). The reducing treatment in hydrogen at 620 K results in FW => EFW removal for significant part of iron, 51 % of spectral area can be assigned to Fe^{2+}. These ions are probably located at EFW sites (due to the larger ionic radii they cannot be accomodated in FW sites any more). The proportion of Brønsted acidic Fe^{3+} FW sites (Δ = 1.81 mm/s) decreased to 16 %. The larger portion of Fe^{3+} component exhibit smaller quadrupole splitting (Δ = 1.29 mm/s). This can be attributed to the formation of Fe^{3+}_{FW}-O-Fe^{2+}_{EFW} pairs (Fig. 2c). Fe^{2+} ions are larger, they distort the symmetry around the FW Fe^{3+} ions in lesser extent than H^+ ions do. The final evacuation restores the H^+ charge compensation for 39 % of FW Fe^{3+} iron (Δ = 2.00). The other main Fe^{3+} component can be assigned to iron located in Fe^{3+}_{FW}-O-Fe^{3+}_{EFW} pairs (Fig. 2d). The presented series of spectra illustrates the redistribution of iron ions during treatments. Upon the reducing treatment in hydrogen a significant part of iron was removed from the FW sites EFW ones, and Fe_{FW}-O-Fe_{EFW} pairs were formed. It is worth noticing that reversible redox $Fe^{3+} \Leftrightarrow Fe^{2+}$ transition has taken place only on the extra-framework part of Fe_{FW}-O-Fe_{EFW} dimers, the FW Fe^{3+} has not changed its valency.

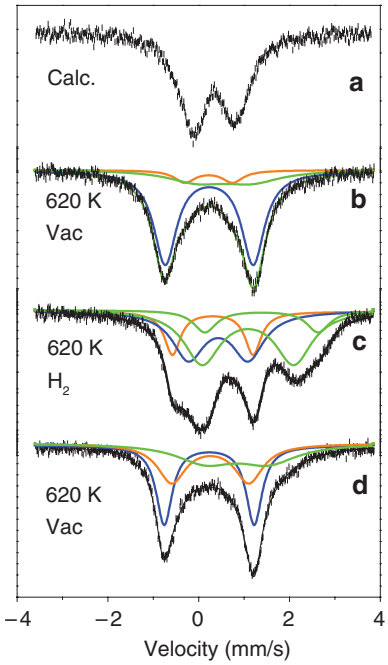

Fig. 2: Series of in situ Mössbauer spectra recorded in sequence after various treatments. (Spectra were recorded at ambient temperature, except spectrum d, 77 K) FW Fe^{3+} contributions are marked in blue, EFW Fe^{3+} in brown and EFW Fe^{2+} in green.

Table 1: Parameters of spectral components shown in Fig. 2.

Treatment	Comp.	δ [a]	Δ [b]	RI [c]
Calc./as rec.	Fe^{3+}	0.33	1.43	33
	Fe^{3+}	0.29	0.56	26
	Fe^{3+}	0.36	0.96	40
Evac.	Fe^{3+}_{FW}	0.23	1.97	72
620 K	Fe^{3+}_{EFW}	0.22	1.01	8
	Fe^{2+}_{EFW}	0.59	1.13	20
H_2	Fe^{3+}_{FW}	0.34	1.81	16
620 K	$Fe^{3+}_{FW/EFW}$	0.44	1.29	33
	Fe^{2+}_{EFW}	1.14	2.03	39
	Fe^{2+}_{EFW}	1.43	2.46	12
Evac.	Fe^{3+}_{FW}	0.23	2.00	39
620 K	$Fe^{3+}_{FW/EFW}$	0.25	1.58	30
	Fe^{2+}_{EFW}	0.89	1.40	32

[a]Isomer shift, mm/s.
[b]Quadrupole splitting, mm/s.
[c]Relative spectral contribution, %.

The Fe-FER sample was evaluated in catalytic processes as well, in oxidation of n-hexane and in hydroxylation of phenol both with hydrogen peroxide in liquid phase. The catalyst was acitve in both reactions promoting the transfer of oxygen by forming hexan-3-one and hydroquinone [17].

(Al + Fe)-FER

The Al : Fe ratio in this sample was 3 : 1, i.e. the probability of formation of Fe_{FW}-O-Fe_{EFW} pairs diminishes, since even the whole amount of iron is not sufficient to provide charge compensation for framework Al^{3+} sites. In situ Mössbauer spectra recorded on this sample after various treatments are shown in Fig. 3.

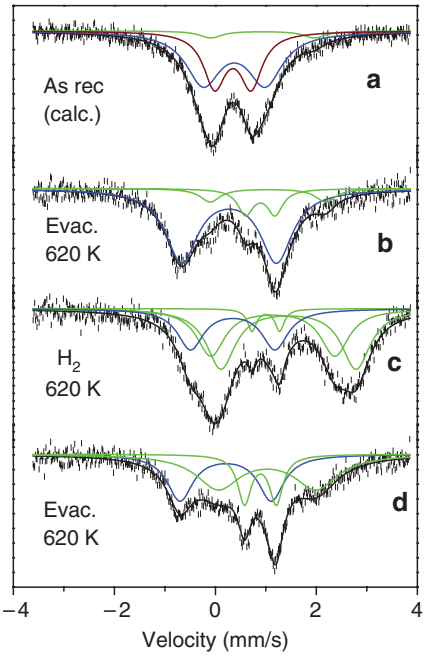

Fig. 3: In situ Mössbauer spectra of (Al + Fe)-FER sample recorded after series of various treatments. (Spectra were recorded at ambient temperature, except spectrum c, recorded at 77 K) FW Fe^{3+} contributions are marked in blue, EFW Fe^{3+} in brown and EFW Fe^{2+} in green.

The shape of spectra recorded after treatments are characteristically different from those of the Fe-FER shown in Fig. 2. The EFW Fe^{3+} is practically absent, except the first spectrum of the calcined component. The first in situ treatment, evacuation of the sample at 620 K C results in the appearance of the Fe_{FW} component, with Brønsted acidic H^+ charge compensation, similarly as was the case with Fe-FER. The subsequent reduction converts ¾ of iron into EFW Fe^{2+} the remainder ¼ is still present as FW Fe^{3+} ($\Delta = 1.67$ mm/s). Remarkable difference in comparison to spectra of the previous Fe-FER sample is the complete lack of the $Fe^{3+}{}_{FW/EFW}$ component assigned to the Fe_{FW}-O-Fe_{EFW} pairs. This lack can be attributed to the dominance of Al ions in those tetahedral sites which require charge compensation by EFW ions (Al : Fe = 3 : 1). The final evacuation does not result in further changes in the distribution of iron among FW and EFW sites. Further data for decomposition of spectra are provided in [17].

The (Al + Fe)-FER sample was tested in the same reactions under the same conditions (oxidation of hexane and phenol) as Fe-FER in the preivious case. The sample did not exhibit any catalytic activity for oxidation. Thus, the comparison of Fe-FER and (Al + Fe)-FER samples shows that the catalytic activity for oxygen transfer in liquid phase oxidations can be attributed to presence of Fe_{FW}-O-Fe_{EFW} pairs, where the $Fe^{2+} \Leftrightarrow Fe^{3+}$ process may proceed on the extra-framework iron component. The aluminum containing counterparts, the Al_{FW}-O-Fe_{EFW} pairs are probably not active in this oxidation.

It might be added that similar redistribution of iron ions were observed on three types of MCM-22 samples, with possible formation of Fe_{FW}-O-Fe_{EFW} pairs ($Fe^{3+}{}_{FW}$ with $\Delta = 1.53$ mm/s) [24]. These Fe-MCM-22 samples were not tested in catalytic processes.

Changes in coordination of iron in mesoporous MCM-41

Channel diameters in mesoporous substances are usually in the 3–7 nm range. These values are larger with c.a. one order of magnitute as compared to microporous zeolites. Walls of channels and pores in mesoporous substances are partly amorphous, crystallinity is less expressed in them than in microporous zeolites [25]. Similarly to zeolites not only silicon, but aluminum, and other transitional metal ions can also be incor-

porated into them, and structural rearrangements may also proceed in the neighborhood of these ions, as well. This feature can clearly be observed on mesoporous ferrisilicates, and can be followed by Mössbauer spectroscopy, too. As an illustration a series of in situ Mössbauer spectra recorded on Fe-MCM-41 ferrisilicate exposed to a sequence of treatments at different conditions is presented and interpreted below (Fig. 4).

The first calcination was performed at 750 K (Fig. 4a). The subsequent evacuation at 670 K results in a Fe^{3+} => Fe^{2+} autoreduction in a considerable extent, c.a. 1/3 of iron is reduced to Fe^{2+}. The most significant part of the spectrum (44 %) can be attributed to Fe^{3+} located in tetrahedral coordination. However, this siting is not characteristic for crystalline FW sites as was the case for microporous Fe-FER and Fe-MFI. Namely, in the subsequent spectrum recorded in a stream of hydrogen at 620 K almost all the iron is present in Fe^{2+} oxidation state (except 8 %, Fig. 4c). This is in strong contrast with the properties of microporous Fe-FER and Fe-MFI samples where the FW Fe^{3+} maintained its ferric state at this condition. This clearly shows the flexibility of the mesoporous structure, i.e. that the reducing hydrogen have access to almost all the ferric iron ions present in this substance previously. The following evacuation does not influence the dominance of ferrous state (Fig. 4d). A repeated 10 h long calcination at 670 K has certain influence on the structure, the proportion of the tetrahedrally coordinated Fe^{3+} component increases to 60 %. The 7th spectrum of this series was recorded in a stream of CO at 570 K. Tetrahedrally coordinated Fe^{3+} is present in 18 %, the other speces are in ferrous state. Thus the extent of the involved proportion in the Fe^{3+} => Fe^{2+} reduction depends on the reducing component, too, (in hydrogen only 8 % retained the Fe^{3+} state, Fig. 4c). The fourth, final evacuation shows a restructured system. The contribution of the tetrahedral Fe^{3+} component reaches almost ½ part of the spectral area, the remaining other ½ part is shared between Fe^{2+} species. Thus, this series of spectra clearly illustrates the high flexibility of the MCM-41 mesoporous structure, the openness of iron ions for changes both in their coordination and oxidation states. Further details of interpretation of spectra can be found in [20].

It is worth mentioning that these Fe-MCM-41 catalysts have been tested in CO oxidation. They did not exhibit catalytic activity if they were pretreated at temperatures only below 620 K. In contrast, they exhibit good activity in the CO oxidation already at ca. 350 K, provided they were exposed to reducing pretreatment at 770 K or at higher temperatures [26]. This demonstrates that he original amorphous structure is not sufficient to exert the catalytic effect yet. In order to provide the appropriate performance further rearrangements and stabilizations are necessary. The presented series of spectra attests that the Fe-MCM-41 is able for a variety of structural changes, and a catalytically efficient one can be formed, however, the active structure may also be subject to profound changes.

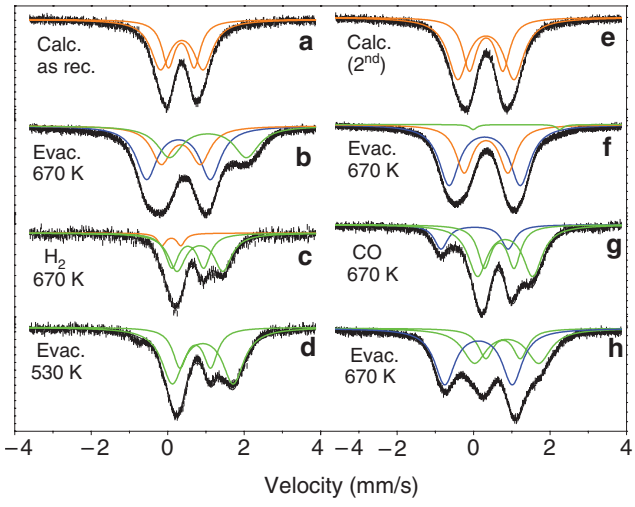

Fig. 4: In situ Mössbauer spectra of Fe-MCM-41 in a series of subsequent treatments. Contrubutions of Fe^{3+} in octahedral coordination are marked in orange, Fe^{3+} in tetrahedral in blue, Fe^{2+} in green. Most of spectra were recorded at ambient temperature, except spectra c (620 K), d (530 K), g and h (both 570 K).

Relocation of iron with partial damage of lattice - catalytic activity retained in decomposition of N_2O

Fe-MFI with FW and EFW iron in N_2O decomposition at different temperatures

Presence and participation of various iron species in decomposition of a greenhouse gas, N_2O, has been the objective of several studies (recently e.g. [27]). Most of studies ascribe the catalytic activity to Fe^{2+} species,[8, 9], other studies suggest the assignment of the catalytic activity to dinuclear EFW centers similar to those shown in Fig. 1. [28, 29]. In our related study an Fe-MFI sample was synthesized into which both FW and EFW iron components were introduced intentionally, thus formation of Fe_{FW}-O-Fe_{EFW} pairs was facilitated. First FW $^{57}Fe^{3+}$ was inserted in a hydrothermal synthesis (Si/^{57}Fe ~ 200), then EFW Fe^{2+} was added by impregnation from ethanolic solution of $FeSO_4$. The preparation was successful, doublets for both the Fe^{3+} and Fe^{2+} components were present after an evacuation at 670 K (Fig. 5a). To check whether the Fe^{2+} component can be stabilized in N_2O atmosphere at higher temperatures an in situ spectrum was recorded in a stream of N_2O at 520 K. Surprisingly, the Fe^{2+} component was still present in this strong oxidizing atmosphere at this elevated temperature (Fig. 5b). The spectrum recorded after the treatment (not shown) is very similar to that shown in Fig. 5a. Thus, it can be concluded that the structure and proportions between Fe^{2+} and Fe^{3+} oxidation states have not been changed in this Fe-MFI up to temperature of 670 K (the temperature of evacuation).

Activation of iron species is described in most of communications to develop catalytic activity in the N_2O decomposition process. Usually a high temperature treatment is proposed in inert atmosphere. To comply with this condition our Fe-MFI sample was heated to 770 K in He stream and was conditioned for 2 h. After

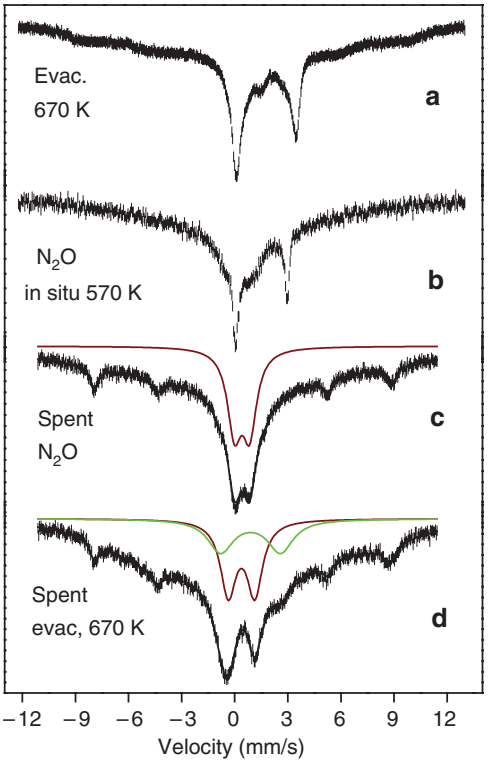

Fig. 5: Mössbauer spectra of (Fe^{2+}/Fe^{3+}) Fe-MFI. (a) After hydrothermal insertion of FW $^{57}Fe^{3+}$, subsequent impregnation with $FeSO_4$ and evacuation. Measured at 77 K. (b) In situ measurement in N_2O at 520 K. (c) and (d): After temperature programmed reaction test, both spectra measured at 77 K. (c) Kept in N_2O during cooling, (d) after subsequent removal of N_2O with evacuation. Fe^{3+} shown in brown, Fe^{2+} in green. Contribution from oligomeric iron is omitted for clarity.

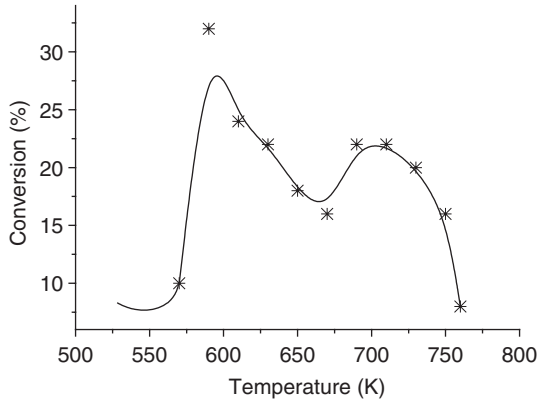

Fig. 6: Activity of the Fe-MFI catalyst in the temperature programmed decomposition of N_2O [19].

cooling the catalytic activity was tested in a temperature programmed reaction (10 % N_2O in He, 5 K/min ramp). The Fe-MFI catalyst was active in the 570–750 K temperature range, as shown in Fig. 6. Two local maxima appear, the first around 600 K, the second, with lesser intensity at 690–730 K.

Mössbauer spectra were also colleced on the spent catalyst. First the catalyst was simply cooled in N_2O and measured at 77 K (Fig. 5c). Broad relaxing component and magnetically ordered sextet are displayed. These components can be attributed to various Fe_xO_y oligomers, which may be accommodated in the channels of MFI structure as illustrated in the upper right corner of Fig. 1b. The remaining significant part in the center of spectrum with 20 % contribution is a doublet which can clearly be attributed to Fe^{3+} ions ($\delta_{77\,K} = 0.41$ mm/s, and $\Delta_{77\,K} = 0.86$ mm/s, marked with brown in Fig. 5c). To check whether there exist possibility for $Fe^{3+} <=> Fe^{2+}$ reversal on the spent catalyst an evacuation was performed at 670 K. The obtained spectrum is shown in Fig. 5d. Surprisingly, the removal of sorbed N_2O resulted in the appearance of an Fe^{2+} component as well. Beside the relaxing and magnetically split oligomeric Fe^{3+} components, doublets of Fe^{2+} ($\delta_{77\,K} = 0.89$ mm/s, and $\Delta_{77\,K} = 3.38$ mm/s), and Fe^{3+} ($\delta_{77\,K} = 0.38$ mm/s, and $\Delta_{77\,K} = 1.50$ mm/s) can clearly be distingiushed with roughly similar share of contributions 13 % and 18 %, respectively. Thus, the spent catalyst, which was heated up to 860 K in the test of temperature programmed reduction was still able to exhibit the feature of $Fe^{3+} \Leftrightarrow Fe^{2+}$ reversal. It is worth to recall that Fig. 5 exhibits two local maxima in the N_2O decomposition process. The first maximum can probably be related to catalytic centers with dominant presence of Fe^{3+}_{FW}-O-Fe^{2+}_{EFW} pairs as can be deduced from Mössbauer spectra shown in the upper part of Fig. 5. The second activity peak in the decomposition may probably be related a partly damaged catalyst structure, as formation of Fe_xO_y oligomers can be detected. However, the ability for $Fe^{3+} \Leftrightarrow Fe^{2+}$ reversal is still present on similar proportions of iron ions. Thus, presence of Fe^{3+}_{FW}-O-Fe^{2+}_{EFW} pairs on this restructured catalyst cannot be excluded either. Further details on the studies of N_2O decomposition with the (Fe^{2+}/Fe^{3+}) Fe-MFI catalyst are described in [19, 30].

Conclusions

Rearrangement of iron ions in various microporous and mesoporous ferrisilicates during redox treatments have been demonstrated. Coexistence of FW Fe^{3+}, EFW Fe^{3+} and EFW Fe^{2+} was observed. Formation of combined FW/EFW dinuclear μ–oxo Fe_{FW}-O-Fe_{EFW} centers is suggested in microporous Fe-FER and Fe-MFI samples. The suggested presence of these μ-oxo centers is in good correlation with catalytic actvity shown in corresponding oxygen transfer processes. Restructurization in the vicinity of iron ions located in flexible pore walls of mesoporous Fe-MFI-41 can also be revealed. This rearrangement results in the development of a more ordered structure, which is also reflected in the improvement of catalytic effect for CO oxidation.

References

[1] P. A. Jacobs, M. Tielen, J-P. Linart, J. B. Uytterhoeven, H. Beyer. *Faraday Trans. I,* **72**, 2793 (1976).
[2] Y. Itho, S. Nishiyama, S. Tsuruya, M. Masai. J. Phys. Chem. **98**, 960 (1994).
[3] P. A. Jacobs. *Stud. Surf. Sci. Catal*. **29**, 357 (1986).
[4] M. R. Mihályi, Á. Szegedi, F. Lónyi. in *Silica and Silicates in Modern Catalysis*, I. Halász (Ed.), pp. 213–255, Transworld Research Network, Trivandrum (2010).
[5] E. J. M. Hensen, E. A. Pidko, N. Rane, R. A. van Santen. in *From Zeolites to Porous MOF Materials*. R. Xu, Z. Gao, J. Chen, W. Yan, (Eds.), Studies in Surface Science and Catalysis, Vol. 170 B. pp. 1182–1189 (2007).
[6] J. Čejka, N. Žilková, P. Nachtigall, (Eds.) Molecular Sieves: From Basic Research to Industrial Applications, *Studies in Surface Science and Catalysis*, Vol. 158. (2005) Elsevier Communications therein.
[7] Md. A. Uddin, T. Komatsu, T. Yashima. *J. Catal.* **146**, 468 (1994).
[8] B. E. R. Snyder, P. Vanelderen, M. L. Bols, S. D. Hallaert, L. H. Böttger, L. Ungur, K. Pierloot, R. A. Schoonheydt, B. F. Sels, E. I. Solomon. *Nature* **536**, 317 (2016).
[9] A. Zecchina, M. Rivallan, G. Berlier, C. Lamberti, G. Ricchiardi. *Phys. Chem. Chem. Phys*. **9**, 3483 (2007).
[10] P. J. Smeets, J. S. Woertink, B. F. Sels, E. I. Solomon, R. A. Schoonheydt. *Inorg. Chem.* **49**, 3573 (2010).
[11] G. D. Pirngruber. in *Ordered Porous Solids*, V. Valtchev, S. Mintova, M. Tsapatsis (Eds.), pp. 749–770, Elsevier, Amsterdam, The Netherlands (2009).
[12] L. Capek, V. Kreibich, J. Dedecek, T. Grygar, B. Wichterlova, Z. Sobalik, J. A. Martens, R. Brosius, V. Tokarova. *Microporous Mesoporous Mater.* **80**, 279 (2005).
[13] K. Lázár, A. N. Kotasthane, P. Fejes. *Catal. Lett*. **57**, 171 (1999).
[14] P. Sazama, B. Wichterlova, E. Tabor, P. Stastny, N K. Sathu, Z. Sobalik, J. Dedecek, S. Sklenak, P. Klein, A. Vondrova. *J. Catal.* **312**, 123 (2014).
[15] K. A. Dubkov, N. S. Ovanesyan, A. A. Shteinman, E. V. Starokon, G. I. Panov. *J. Catal.* **207**, 341 (2002).
[16] J. B. Taboada, A. R. Overweg, M. W. J. Craje, I. W. C. E. Arends, G. Mul, A. M. van der Kraan. *Microporous Mesoporous Mater*. **75**, 237 (2004).
[17] K. Lázár, G. Lejeune, R. K. Ahedi, S. S. Shevade, A. N. Kotasthane. *J. Phys. Chem. B,* **102**, 4865 (1997).
[18] P. Fejes, I. Kiricsi, K. Lázár, I. Marsi, A. Rockenbauer, L. Korecz, J. B. Nagy, R. Aiello, F. Testa. *Appl. Catal. A*, **242**, 247 (2003).
[19] K. Lázár, O. Pozdnyakova, A. Wootsch, P. Fejes. *Hyperfine Interact*. **167**, 779 (2006).
[20] K. Lázár, G. Pál-Borbély, Á. Szegedi, H. K. Beyer. *Stud. Surf. Sci. Catal*. **142**, 1347 (2002).
[21] R. G. Burns. *Hyperfine Interact.* **91**, 739 (1994).
[22] R. G. Burns. in *Mixed Valence Systems: Applications in Chemistry, Physics and Biology*. K. Prassides, (Ed.) NATO ASI-C Ser. Mat. Phys. Sci., C **343, 175** (1991).
[23] K. Lázár, K. Matusek, J. Mink, S. Dobos, L. Guczi, A. Vizi-Orosz, L. Markó, W. M. Reiff. *J. Catal*. **87**, 163 (1984).
[24] R. M. Mihályi, K. Lázár, M. Kollár, F. Lónyi, G. Pál-Borbély, Á. Szegedi. *Microporous Mesoporous Mater*. **110**, 51 (2008).
[25] S. Schacht, M. Janicke, F. Schüth. *Microporous Mesoporous Mater.* **22**, 485 (1998).
[26] Á. Szegedi. *Physico-chemical properties of mesoporous silicates containing transition metals*. PhD Theses, University of Szeged (2004).
[27] M. Rutkowska, L. Chmielarz, M. Jablonska, C. J. Van Oers, P. Cool. *J. Porous. Mater* **21**, 91 (2015).
[28] R. Joyner, M. Stockenhuber. *J. Phys. Chem. B* **103**, 5963 (1999).
[29] A. L. Yakovlev, G. M. Zhidomirov, R. A. van Santen. *J. Phys. Chem. B* **105**, 12297 (2001).
[30] L. Guczi, K. Lázár. *React. Kinet. Catal. Lett*. **96**, 335 (2009).